Preprints of the 18th IFAC World Congress
Milano (Italy) August 28 - September 2, 2011

Control of a Magnetic Capture Device for Autonomous In-orbit Rendezvous

S. Clerc*, H. Renault*, D. Losa*

**Thales Alenia Space, 100 Bd du Midi, Cannes la Bocca, France*
(Tel: +33-49292 6052; e-mail: {Sebatien.Clerc,Herve.Renault}@ ThalesAleniaSpace.com).

Abstract: Mission concepts proposed to return Mars soil samples to Earth involve a critical rendezvous phase with a passive sample container placed in Mars orbit by an ascent vehicle. An innovative magnetic capture device was recently proposed to increase the reliability and simplify capture operations. The present paper presents control aspects of this device. More specifically, the magnetic capture devices allows to damp rotation rates and to enforce a specific relative orientation of the sample container at a range of about 4 meters. The final contact is secured thanks to a additional, small, passive magnet. The linear stability and performance of the controller is analyzed, and non-linear simulations are presented.

Keywords: Interplanetary Spacecraft, Space Robotics, Magnetic fields.

1. INTRODUCTION

Sampling and returning to Earth a small mass of Martian soil for analyses is a one of the most exciting objectives in the study of the Solar System. Mars Sample Return (MSR) mission concepts have been studied for years by NASA (D'Amario et al., 1999), CNES (Cazaux et al., 2004) and ESA. All concepts involve in orbit rendez-vous operations around Mars between a vehicle carrying the Martian sample (target) and an Earth-return spacecraft (chaser). The soil samples need to be transferred safely from one vehicle to the other.

A major trade-off at this point concerns the capability of the target vehicle. A first option considers a vehicle with attitude control capabilities, allowing a soft docking with the return spacecraft. A second option considers a simpler uncontrolled vehicle which is captured by the chaser. In this option the target is reduced to a small spherical container (the Sample Container, SC), possibly equipped with navigation supporting devices such as laser retro-reflectors and RF beacons. Pros and cons of both strategies are recalled in Table 1.

The capture option has several drawbacks, the most critical ones being the increased complexity of the sample transfer mechanism (since the orientation of the Sample Container can be arbitrary), and the lack of robustness. The capture device must first be deployed (first single point failure mode). When the SC enters the capture device, a mechanism is activated to prevent it from exiting again. The activation is in principle irreversible, so only one attempt is allowed (second single point failure mode). The deployment and the activation of the capture may each require several minutes, which makes a ground validation in simulated weightlessness conditions problematic.

The docking option involves a significant mass penalty for the target vehicle. The mass budget is extremely critical for this vehicle because of the enormous snow-ball factor arising from the combination of Earth escape, Mars landing and Mars ascent. For this reason, most trade studies performed so far concluded in favor of the capture option in spite of its drawbacks.

Table 1. Comparison of docking, capture and magnetic capture options for a Mars Sample Return mission.

	Docking	**Capture**	**Magnetic Capture**
Target attitude control system	Active	None	Passive
Target docking system	Yes	No	Yes
Overall Target mass	High	Minimal	Low
Chaser control system	6-dof	6-dof	6-dof + magnetic
Chaser Capture / docking system	Simple	Complex	Simple
Sample transfer system	Translation	Rotation + Translation	Translation
Overall Chaser mass	Low	High	Medium
Reliability of capture and transfer	High	Low	High
Multiple attempts & Reversibility	Yes	No	Yes
Heritage	Large	No	No

However a new concept based on a magnetic capture and docking device has been proposed recently (Renault et al.,

2008) which provides some of the advantages of the docking solution but with a mass budget comparable to the capture option. In particular, the magnetic capture device allows controlling the rotation rate and the orientation of the target vehicle, and ensures a robust and reversible docking to the chaser vehicle. The reversibility of the docking system implies the crucial possibility to perform several attempts in case of failure, and authorizes unconventional mission architecture options (e.g. transfer to a third vehicle or return to Earth without transfer).

The purpose of the present paper is to provide a preliminary demonstration of the feasibility of the concept from a control point of view. The concept also raises a number of system-level issues, such as the compatibility of the concept with system mass and power budgets of the orbiter and SC or with the magnetic integrity of the soil samples, as well as accommodation and mechanical issues. These points have been studied independently but are outside the scope of this paper.

2. MAGNETIC CAPTURE PRINCIPLES AND PHASES

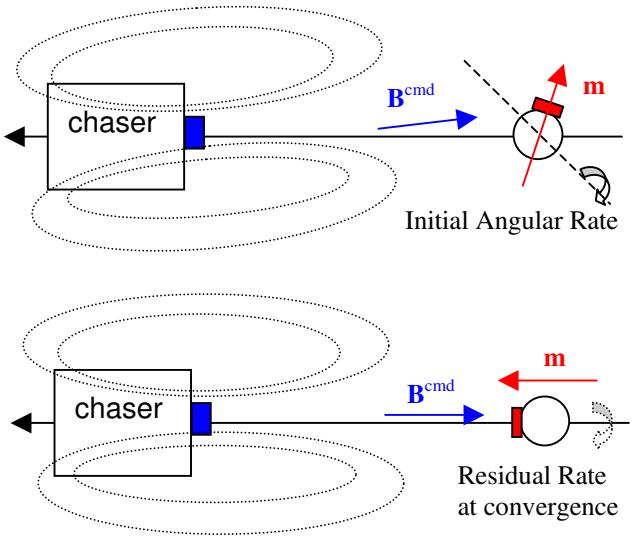

Figure 1: Magnetic attitude control principle. Top: initial situation. Bottom: stabilized rotation at convergence.

The magnetic capture concepts requires some specific equipment. First, the SC is equipped with a permanent magnet aligned with the capture axis. The SC also features a docking port. The Orbiter GNC includes on the other hand magneto-meters to sense the orientation of the SC dipole, and magneto-torquers to control its orientation. Additionally, a small magnet can be placed on the chaser docking port to secure the docking.

The magnetic capture process comprises three main phases: an attitude control phase at a station keeping point, a closing phase, an a short free drift and docking phase.

The attitude control phase lasts approximately 4000 s. During this phase, the chaser spacecraft performs station keeping at a fixed distance of 4 meters approximately along the rendezvous axis. The magnetic control scheme reduces the rotation rate of the SC and orients the docking side in the proper direction.

At this point the closing and docking operations can start. From the GNC point of view, they are similar to those envisaged for a standard mechanical capture. The chaser spacecraft accelerates to reach a constant closing velocity of 5 cm/s. The magnetic attitude control is no longer necessary and it is progressively phased out. Indeed the closing phase is short enough (100 s) to ensure that the orientation of the SC remains correct without further control.

During the final meters of the capture, the control is hindered by limitations on the sensor operation range and possible thruster plume interactions. Therefore the final part of the trajectory (1.5 to 3 meters depending on spacecraft characteristics) is performed in free drift. The scenario ends with the contact of the SC and orbiter docking ports.

4. MAGNETIC ATTITUDE CONTROL LINEAR STABILITY

As explained above, the magnetic attitude control phase performs two functions: rate damping and SC orientation control.

The first function is required to damp the angular rate acquired by the SC when it is placed into orbit by the Mars ascent vehicle. The initial angular rate results from the Mars ascent vehicle residual rotation rate at separation plus those introduced by the separation mechanism. It is estimated that the rates can reach 20 °/s in a worst case situation.

The rate damping process is similar to magnetic control schemes used for LEO spacecraft (see e.g. Beaupellet et al., 2007, Zentgraf and Reggio, 2009). In absence of significant external torques acting on the SC, a simple proportional feedback is enough. The applied magnetic field in the chaser frame is proportional to the measured rate of change of $\mathbf{m}$, the SC dipole magnetic momentum, as measured by the chaser magnetometers. Let $\dot{\mathbf{m}}_{chaser}$ denote this measurement. The second function achieved by a constant magnetic field in the chaser frame. We will call this controller the precession controller since it creates a precession of the SC rotation axis.

The total magnetic field in the chaser frame is a sum of these two controllers:

$$\mathbf{B}_{chaser}^{cmd} = \mathbf{B}^0 - K_d \dot{\mathbf{m}}_{chaser} \tag{1}$$

Here $\mathbf{B}^0$ is the constant field of the precession controller, K_d is the gain of the rate damping controller.

In order to analyze the behaviour of the controller, we write the equations of the motion of the SC in body-fixed frame:

$$\begin{cases} \mathbf{I}\dot{\boldsymbol{\omega}} + \boldsymbol{\omega} \times \mathbf{I}\boldsymbol{\omega} = \mathbf{m} \times \mathbf{B}_{SC}^{cmd} = \mathbf{m} \times \left(-K_d \boldsymbol{\omega} \times \mathbf{m} + \mathbf{B}_{SC}^0 \right), \\ \dot{\mathbf{B}}_{SC}^0 + \boldsymbol{\omega} \times \mathbf{B}_{SC}^0 = 0. \end{cases} \tag{2}$$

The subscript *SC* denotes the value of a vector in the SC-fixed frame.

It is clear that under the effect of the controller, the total rotational energy of the SC is non-increasing. However no control can be exerted around the direction of the fixed magnetic momentum of the SC, so the rotation rate cannot be completely cancelled.

We assume at this point that the magnetic moment vector $\mathbf{m}$ is aligned with a principal axis of inertia, e.g. the Z axis: $\mathbf{m} = (0,0,m)$. A constant rotation around this axis has no effect on the rate damping controller $\mathbf{B}_{inertial}^{cmd} = -K_d \dot{\mathbf{m}}_{inertial}$. If moreover the Z body axis is aligned with the constant magnetic field $\mathbf{B}^0$, the precession controller is also inactive, and $\boldsymbol{\omega} = (0,0,\Omega)$ is a steady-state solution of system (2).

In order to analyze the stability of this solution, we linearize equation (2) around $\boldsymbol{\omega} = (0,0,\Omega)$, $\mathbf{B}_{SC}^0 = (0,0,-B^0)$. The equations for the Z components of the vectors are trivial and decoupled, so we consider only the X and Y components:

$$\frac{d}{dt}\begin{pmatrix} I_x\omega_x \\ I_y\omega_y \\ b_x^0 \\ b_y^0 \end{pmatrix} + \begin{pmatrix} K_d m^2 & (I_z - I_y)\Omega & 0 & -m \\ (I_x - I_z)\Omega & K_d m^2 & m & 0 \\ 0 & B^0 & 0 & \Omega \\ -B^0 & 0 & -\Omega & 0 \end{pmatrix} \cdot \begin{pmatrix} \omega_x \\ \omega_y \\ b_x^0 \\ b_y^0 \end{pmatrix} = 0 \qquad (3)$$

The stability of system (3) is difficult to study analytically in general, but the case without precession control ($B^0 = 0$) brings some useful insight.

If the Z axis is an axis of major or minor inertia, the system may have either a pair of complex conjugate eigenvalues with negative real part, or two negative real eigenvalues. In both cases the system (3) is linearly stable for any value of Ω. This means that arbitrary large rotation rates can be encountered.

If on the other hand the Z axis is an intermediate axis of inertia, the eigenvalues of the system are always real. They are both negative if and only if:

$$\Omega < K_d m^2 \Big/ \sqrt{(I_x - I_z)(I_z - I_y)} \qquad (4)$$

This means that stable steady-state solutions are possible only if Ω is small. Although a null angular rate cannot be achieved, the controller provides a bound on the steady-state angular rate.

In the case with both rate damping and precession control, the stability of the system can be investigated numerically, by computing the eigenvalues of the closed-loop system (3). The numerical results show that:

- For the minor inertia axis case, the system is linearly stable except for a range of rotation rates
- For the intermediate axis case, the system is linearly stable only for small rotation rates and if the product B_0.m is positive. If B_0.m is negative, the system is unstable for any rotation rate.
- For the major axis case, the system is always stable.

The situation is therefore the same as for the $B^0 = 0$ case, except for the minor axis configuration which is destabilized by the precession control in a band of rotation rates.

To conclude, the study shows that it is critical to align the SC dipole with the intermediate axis of inertia in order to limit the maximum stable rotation rate.

5. SYSTEM SIZING

Equation (4) shows that the lower the control gain K_d, the higher the limit angular rate. On the other hand the characteristic decay time of the kinetic energy is given by $\tau = I_{\max} / K_d m^2$. The lower the control gain K_d, the longer the stabilization takes.

It is therefore possible to trade stabilization time τ against limit angular rate Ω. However in practice it is not desirable to have a stabilization time much longer than a fraction of the orbital period. A typical value for τ is 1000 s.

The product $\Omega\tau = I_{\max} / \sqrt{(I_x - I_z)(I_z - I_y)}$ is a measure of the efficiency of the magnetic rate damping. It depends only on the inertia matrix of the body.

Let us consider as a parameter $\lambda = (I_{min}+I_{mid})/I_{max}$, $1 < \lambda < 2$. Lambda is a measure of the flatness of the body: the case $\lambda = 1$ corresponds to a flat body (optimal from control point of view but not structurally feasible), $\lambda = 2$ is the spherical case (optimal packing factor but worst case from control point of view). It is possible to show that for a fixed value of λ, the product Ωτ is minimal if the inertia matrix is given by: (λ/2, 1 , ½ + 1/λ).

Figure 2 shows the residual rotation rate Ω (in °/s) as a function of the parameter λ, for a given time constant τ of 1000 s. A target maximum rate can be achieved by enforcing the corresponding value for the geometrical parameter λ. This can be achieved by placing the components in a an appropriate way inside the SC, a the cost of an increase of the SC envelope.

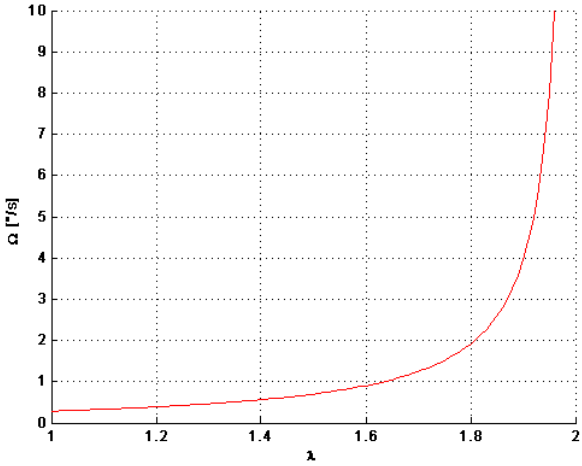

Figure 2: Residual rotation rate of the SC, as a function of the flatness parameter λ. λ = 1 corresponds to a flat body, λ = 2 to a spherical body.

We consider in the following a value of λ = 1.5, which ensures a limit rotation rate below 0.7 °/s. This inertia

corresponds for instance to the case of an homogenous ellipsoid with radii a = 16 cm, b = 20 cm and c = 25 cm. This ellipsoid has the same volume than a sphere of radius 20 cm, with an external envelope (25 cm) that is only 25% larger.

Another important aspect concerns the sizing of the magnetic actuator and the SC dipole moment. It is obviously linked to the distance between the SC and the orbiter (a smaller distance allows using smaller actuators). This distance is limited by the ability to perform station-keeping at close range, because of sensor minimal operating ranges and potential thruster plume interactions.

The magnetic dipoles of the SC and the orbiter must be large enough to avoid saturation at the beginning of the rate-damping process. The required torque depends on the expected worst case initial rotation rate of the SC ω_0, here 20 °/s. The actuators are not saturated if:

$$3\frac{\mu_0}{4\pi} m_{SC} m_{orb} \frac{1}{r^3} \geq \frac{I.\omega_0}{\tau}$$

This is ensured if m_{SC} = 100 Am², m_{orb} = 400 Am², and r = 4 m. These values are within current technological capabilities (for permanent magnet, magneto-torquer and station-keeping GNC).

6. SENSING AND NOISE CONSIDERATIONS

6.1 Sensing

The rate-damping control scheme (1) requires the knowledge of $\dot{\mathbf{m}}$, the time-derivative of the magnetic dipole of the SC, measured in the orbiter frame. This quantity is not measured directly and must be recovered from the magnetic field measurement by a 3-axis magnetometer.

The magnetic field induced by a magnetic dipole **m** is given by the classical formula:

$$\mathbf{B} = \frac{\mu_0}{4\pi}\frac{1}{|\mathbf{u}|^3}\left(3(\mathbf{m}.\mathbf{u})\,\mathbf{u} - \mathbf{m}\right)$$

Indeed this linear relation can be easily inverted to get an estimate of the magnetic momentum using a measurement of the magnetic field (provided that the relative position vector u is known)

$$\mathbf{m} = \frac{4\pi}{\mu_0}|\mathbf{u}|^3\left(\frac{3}{2}(\mathbf{B}.\mathbf{u})\,\mathbf{u} - \mathbf{B}\right) \qquad (5)$$

This relation is used to estimate the current orientation of the OS magnetic sample using the measurement of a magnetometer.

Similarly, the rate damping scheme (1) expresses the control magnetic field $\mathbf{B}_{cmd}$ to apply on the SC, and this vector must be related to the magnetic dipole command vector $\mathbf{m}_{cmd}$. This involves again equation (5).

Numerical simulations show that the control scheme is robust to uncertainties on the knowledge of the position vector u of several centimetres.

Magnetic actuation and sensing cannot be efficiently performed simultaneously, so a duty-cycle needs to be established, leaving e.g. 10% of the time for sensing. This is a standard practice for spacecraft magnetic control.

Finally, one must consider the impact of sensing noise on the performance of the control. Indeed the typical magnetic field signal from the SC measured is quite small: typically 150 nT. Magnetic disturbances from spacecraft hardware are of the same order of magnitude for a conventional spacecraft, although a careful design could probably bring them one order of magnitude lower.

Finally, one must consider the effect of Mars' magnetic field. This point is addressed in detail in the next paragraph.

In any case, a pre-filter is required to reduce the sensing noise, particularly because the signal must be differentiated (cf. equation 1).

A simple 2nd order low pass filter has been considered:

$$H(s) = \frac{0.25}{s^2 + \sqrt{0.5}s + 0.25}$$

The bandwidth at 0.5 rad/s is compatible with the expected maximum angular rate (0.35 rad/s).

An possible alternative could be to use a dynamic Kalman filter to estimate the orientation of the SC magnetic dipole. Indeed the characteristics of the SC are quite well known and the disturbance torques are low, which allows an accurate modelling of the dynamic.

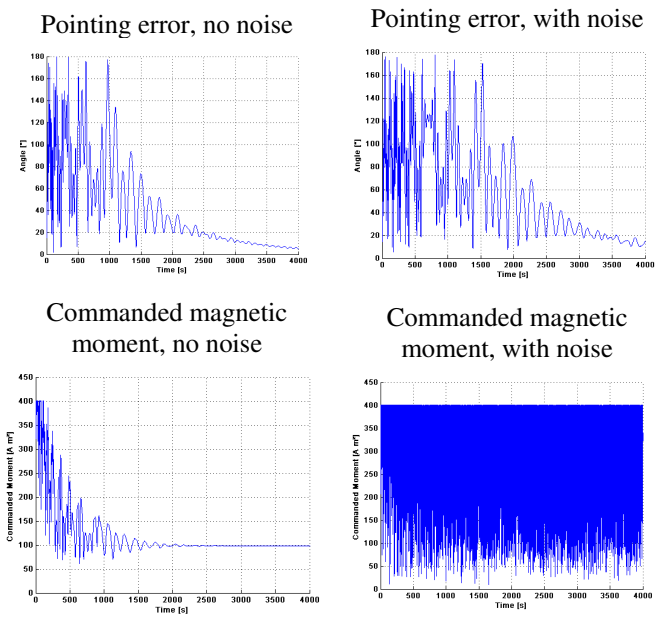

Figure 3: Comparison of magnetic controller behaviour, with and without noise. The effect remains small on the pointing performance (top row) while it is clearly noticeable on the actuation (bottom row).

The effect of the noise has been investigated through numerical simulations, see Figure 3. The top row compares the pointing error, defined as the angle between the SC Z axis

and the nominal capture axis. The bottom row compares the commanded magnetic moment. The results show little degradation of the pointing performance, but the noise is clearly visible on the commanded magnetic moment.

6.2 Mars magnetic field

Mars has a residual magnetic field, with a maximum localized near the surface around a longitude of 180° East and a latitude of 60° South. The peak value, measured by MGS at 400 km of altitude, is around 200 nT. The peak value that will be encountered on the MSR rendezvous orbit will be notably lower because of the higher altitude (500 km) and lower inclination (45°). Nevertheless the value of the disturbance will be comparable to the measured signal from the SC dipole sensed by the Orbiter and the control field sensed by SC. This can result in a alignment error of several degrees.

The proposed approach to this issue is to calibrate the Mars magnetic field in orbit. The measured magnetic field profile as a function of the anomaly should be stored in an-board table and then subtracted from both measurements and control command.

The calibration process should involve a passive measurement along the reference orbit at a distance of e.g. 50 meters from the SC. The distance shall be large enough to minimize the signal from the SC and small enough to ensure that the magnetic field measured by the Orbiter is essentially the same as the one sensed at the SC location. Several orbits may be necessary to obtain a good estimation.

The residual error from the calibration process may be considered as a high-frequency noise. In the simulations, we have considered a white noise with a standard deviation of 30 nT acting on the SC.

7. NUMERICAL SIMULATIONS

In this section, we present some end-to-end simulations of the magnetic capture scenario.

The simulation starts with the magnetic attitude control phase (rate damping and orientation) lasting 4000 s. During this time, the Orbiter GNC performs a station-keeping 4 meters away from the SC on the V-bar. A simplified model of the position control scheme has been implemented in order to check the influence of the position knowledge and control errors on the magnetic control process, and the ability of the position control scheme to compensate the magnetic force disturbance acting on the SC. The position control model includes the effect of relative navigation sensor noise: 1 cm (1 s) on position and 1 mm/s (1 s) on velocity at 10 Hz. The controller performance is also affected by the thruster minimum impulse bit (equivalent to 0.13 mm/s). For the sake of simplicity, the orbital dynamics has not been implemented (free space only) but we do not expect a significant impact on the behaviour of the magnetic and position controllers.

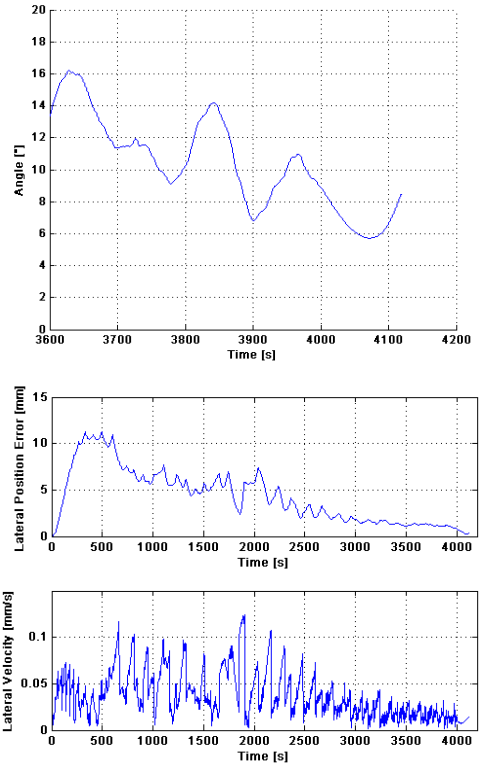

Figure 4: Performance of the magnetic capture concept. Top: close-up of the attitude error at capture time. Bottom: lateral position and velocity errors.

After 4000 s, the SC rotation rate has been successfully reduced and its docking side points roughly toward the Orbiter with a typical precision of 12°. The closing phase is then initiated. The position controller commands a closing velocity of 5 cm/s. The magnetic control is phased out as the distance reduces by reducing the gain. The simulation shows that the alignment error does not change significantly during the short closing phase.

The simulation results presented in Figure 4 show that:

- The magnetic attitude control scheme ensures a docking with an alignment error of the order of 10° only.
- The disturbance introduced by the small magnetic force does not impact the position controller performance. Lateral errors are capture at capture are lower than a few mm in position and 0.1 mm/s in velocity in this simplified simulation.

8. CONCLUSIONS AND PERSPECTIVES

The analyses and simulations presented prove the feasibility of a reversible capture system based on magnetic actuators for an orbital rendezvous with a small object. In particular, we have shown that the concept is robust to the main uncertainties and disturbance sources. The concept provides some critical advantages for the rendezvous and capture phase of a future Mars Sample Return mission: simplification of the design and enhancement of the robustness.

Further work is however required to fully validate the concept. First, some system work should be devoted on hardware implementation and magnetic compatibility issues.

A high-fidelity simulator needs to be developed, in order to handle properly such effects as:

- Mars magnetic field calibration process and residual error
- Fine modelling of orbital translation dynamics and position control; the HARVD simulator (cf. Le Peuvédic et al., 2008) could be used for this purpose
- Impact of the precise localization of the hardware (magneto-meters and magneto-torquers, capture cone, etc.) and spacecraft disturbance sources (e.g. solar arrays, antennas)
- Effect of sensing/actuating duty-cycle
- Fine modelling of the contact dynamics.

The simulator can be used to robustness and sensitivity analyses in a simulated environment, as well as real-time validations using a flight computer, optionally including a stimulated magneto-meter in the loop. Validation on a dynamic test-bench will be more difficult to perform on ground, as is the case for all orbital rendezvous and capture systems. However a possible partial validation could be achieved using a magnetized SC mock-up placed on a 2-degree-of-freedom gimbal system. The behaviour of the docking system itself at short range (a few centimetres) can easily be validated by approaching the Sample Container to the docking pod under various attitudes and incidence angles. Around one second of weightlessness is required to validate the contact dynamics, which is compatible with a ground validation. Further validation options could involve an end-to-end demonstration in Earth or Mars orbit.

REFERENCES

D'Amario, L., Bollman, W., Lee, W., Roncoli, R., Smith, J., Bhat, R., Frauenholz, R., Mars Orbit Rendezvous Strategy for the Mars 2003/2005 Sample Return Mission, AAS/AIAA Astrodynamics Specialist Conference, Girdwood, Alaska, USA, 1999.

Cazaux, Ch., Naderi, F., Whetsel, C., Beaty, D., Gershman, B., Kornfeld, R., Mitcheltree, B., Sackheim, B., The NASA/CNES Mars sample return – a status report, Acta Astronautica, 54, (2004), 601-617.

Renault, H., Arbusti, F., Sainct, H., *Procédé de Capture d'un conteneur d'échantillons de sol planétaire se déplaçant dans l'espace*, INPI Patent Nr. 08 06139, 2008.

Beaupellet, J.-L., Brethé, D., Renaud, P.-Y., Rouat, O., Pirson, L., Tello, M., Landiech, P., PROTEUS platform: JASON-1, CALIPSO and COROT flight results, design evolution, next applications, 30th AAS/AIAA Guidance and Control Conference, Breckenridge, Co., USA, 2007.

Zentgraf, P., Reggio, D., Magnetic Rate Damping of Satellites in LEO, AAS/AIAA 32nd Guidance and Control Conference, Breckenridge, Co., USA, 2009.

Le Peuvédic, C., Colmenarejo, P., Guiotto, A., Autonomous Rendezvous Control System: A high-fidelity Functional Engineering Simulator for GNC/AMM/FDIR Validation, 7th ESA GNC Conference, Tralee, Ireland, 2008.